Journal of Experimental and Theoretical Physics, Vol. 101, No. 3, 2005, pp. 494–503.
Translated from Zhurnal Éksperimental'noĭ i Teoreticheskoĭ Fiziki, Vol. 128, No. 3, 2005, pp. 575–585.

ORDER, DISORDER, AND PHASE TRANSITIONS IN CONDENSED SYSTEMS

Superconducting Current in Hybrid Heterojunctions of Metal-Oxide Superconductors: Size and Frequency Dependences

Yu. V. Kislinskii[a], P. V. Komissinski[a, b], K. Y. Constantinian[a,*], G. A. Ovsyannikov[a], T. Yu. Karminskaya[c], I. I. Soloviev[c], and V. K. Kornev[c]

[a] *Institute of Radio-Engineering and Electronics, Russian Academy of Sciences, Moscow, 125009 Russia*

[b] *Chalmers University of Technology, SE-41296, Göteborg, Sweden*

[c] *Moscow State University, Moscow, 119992 Russia*

**e-mail: karen@hitech.cplire.ru*

Received March 2, 2005

Abstract—We have detected experimentally considerable deviations of the frequency dependences of the Shapiro step amplitudes and the critical current of Nb/Au/$YBa_2Cu_3O_x$ thin-film hybrid Josephson heterojunctions prepared on $YBa_2Cu_3O_x$ metal-oxide superconductor films with a tilted c axis from the regularities inherent in Josephson junctions of traditional superconductors with an s-symmetry of the order parameter. It is shown that possible formation of "splintered" fluxons with a size $\lambda_s < \lambda_J$ due to faceting of the interface and formation of a chain of nanosize 0 and π junctions must be taken into account in describing processes in lumped heterojunctions (whose size L is smaller than the Josephson penetration depth λ_J determined from the averaged value of the critical current density). For heterojunctions with a size $\lambda_s < L < \lambda_J$, a substantial decrease in the maximal amplitude of the first Shapiro step with increasing voltage (Josephson oscillation frequency) is observed at voltages much smaller than the energy gap in niobium ($V \ll \Delta_{Nb}/e$); this effect is manifested most strongly when the size L is greater than λ_s. A fractional Shapiro step and a subharmonic detector response have been observed in the current–voltage characteristics of heterojunctions; the dynamic processes responsible for their emergence and indicating the presence of the second harmonic in the current–phase relation are studied. It is shown that the effect of interface faceting on the current–phase relation increases with a heterojunction size $L > \lambda_s$. © *2005 Pleiades Publishing, Inc.*

1. INTRODUCTION

In most metal-oxide superconductors with a high superconducting transition temperature, the $d_{x^2-y^2}$ symmetry type of the superconducting order parameter dominates (D superconductors) [1, 2]. In Josephson junctions of D superconductors misoriented in the *ab* plane relative to one another, π junctions are formed under certain conditions; for such junctions, the ground state with a phase difference equal to π in the superconducting order parameter is stable [2–9]. In the case of faceting of the interface in Josephson junctions of D superconductors, alternation of 0 and π junctions leads to alternating modulation of the critical current density $j_c(x)$ along the interface on the nanoscale; as a result, pairs of "splintered" fluxons [10] containing a magnetic flux $\Phi_1 < \Phi_0/2$ and $\Phi_2 > \Phi_0/2$, $\Phi_1 + \Phi_2 = \Phi_0$ are formed (Φ_0 is the magnetic flux quantum). Such fluxes were detected experimentally in [11] in bicrystal Josephson junctions D_0/D_{45}.[1] For a large amplitude of spatial variation of the critical current, the size of the splintered fluxon is smaller than the Josephson penetration depth λ_J [10], which provides a new scale of the size dependence of static and dynamic processes in junctions. Fluxons with a fractional magnetic flux quantum were observed in junctions (including those formed by ordinary S superconductors) with inhomogeneities on the order of λ_J [12]. Judging from our earlier preliminary results [4], it cannot be ruled out that such fluxon formations may substantially affect the frequency dependence of dynamic parameters of junctions containing a D superconductor. Theoretical calculations [13] for junctions of D superconductors predict singularities in

[1] In the D_0 superconductor, one of the axes (*a* or *b*) in the basal *ab* plane is directed along the normal to the bicrystal interface (for bicrystal Josephson junctions) or to the plane of the junction (for planar Josephson junctions), while in the D_{45} superconductor, it is turned through an angle of $\theta = 45°$ relative to these axes.

the amplitude of the superconducting current component for gap voltages $V \approx \Delta_D/e$ (Δ_D is the energy gap in a D superconductor) analogous to the Riedel singularity observed in junctions of S superconductors. However, no information is available at present on the frequency dependence of the superconducting current in junctions of D superconductors under voltages much smaller than the superconducting gap.

In Josephson junctions of D superconductors, low-energy bound Andreev states are formed on the (110) plane [2]; these states are clearly manifested in the form of a singularity in the conductivity of junctions at low voltages [2–7, 14] and strongly affect the superconducting current I_s of the junctions. In particular, such states lead to a deviation of the $I_s(\varphi)$ dependence (φ is the phase difference between the wavefunctions of the electrodes of the Josephson junction) from the sinusoidal shape [2–7, 15]. According to the results of theoretical calculations [10, 11], Josephson junctions with an alternating critical current density j_c contain, along with the first harmonic ($\sin\varphi$), the second harmonic ($\sin 2\varphi$). A nonsinusoidal current–phase relation was observed in asymmetric bicrystal Josephson junctions D_0/D_{45} in [8, 16]; we also observed earlier an analogous dependence in hybrid heterojunctions $Nb/Au/YBa_2Cu_3O_x$ prepared on $YBa_2Cu_3O_x$ (YBCO) films with a tilted crystallographic axis c [3]. Note that the second harmonic ($\sin 2\varphi$) was observed in small-size heterojunctions (on the order of tens of micrometers) [3, 17], while deviations from the sinusoidal dependence in larger heterojunctions (on the order of tenths of a millimeter) were not detected [18].[2] It should be noted that the specific growth of a YBCO film tilted at an angle specified by a specially oriented (in the (7 10 2) plane) $NdGaO_3$ substrate is such that facets whose faces are oriented either along the c axis (001) or in the ab plane (110) are formed in the junction region of the heterojunction [4, 19]. Accordingly, it follows from the results of theoretical calculations [2, 5–7] that the transport properties of junctions between such faces and an S superconductor (Nb in our case) must differ substantially, forming alternating nanojunctions of various types (S/D_C and S/D_{45}) in heterojunctions in view of the d symmetry of the order parameter.

Here, we report on the results of experimental investigations of the magnetic field dependences of the superconducting critical current as well as the frequency dependence of the superconducting current and Shapiro steps in Nb/Au/YBCO hybrid heterojunctions on films with a tilted c axis. Assuming the possible formation of fractional fluxons in such heterojunctions and taking into account size limitations [10], we performed experiments on samples with a size L ranging from 10 to 50 μm. The second harmonic amplitude in the current–phase relation is estimated quantitatively and physical mechanisms explaining the experimental data are discussed.

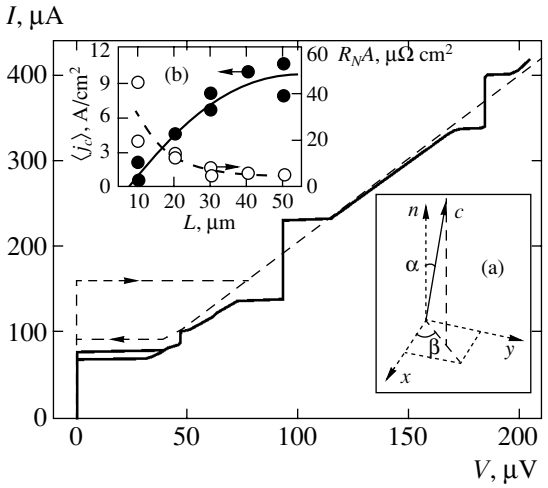

Fig. 1. IV curve of a $Nb/Au/YBa_2Cu_3O_x$ heterojunction with $L = 40$ μm at $T = 4.2$ K: autonomous IV characteristic (dashed curve) and IV characteristic recorded under the action of electromagnetic radiation of frequency $f_e = 43.45$ GHz (solid curve). The direction of the bias current is shown by arrows. Inset (a) is schematic representation of an inclined YBCO film with the (1 1 20) orientation, $\alpha \approx 11°$ and $\beta \approx 45°$. Inset (b) is the dependence of the critical current density $\langle j_c \rangle$ and the characteristic resistance R_NA of the junction on its linear size L (dashed and solid curves are functional dependences providing the best approximation of experimental data).

2. EXPERIMENTAL TECHNIQUE

YBCO epitaxial films with a thickness of 150 nm were deposited by laser sputtering at a temperature of 770–790°C in oxygen under a pressure of 0.6 mbar. For growing YBCO films, we chose $NdGaO_3$ substrates with the (7 10 2) orientation. Detailed studies using X-ray diffractometry revealed that YBCO films formed on the (7 10 2) plane of the $NdGaO_3$ substrate as a result of epitaxial growth have the (1 1 20) orientation, so that the crystallographic c axis is deflected from the normal to the substrate plane through an angle $\alpha \approx 11°$, remaining in the (110) plane of the YBCO film (see inset (a) to Fig. 1). Preliminary investigations proved that a film inclination by 10°–14° is optimal for the electron transport along the ab plane, preserving the monodomain nature of the film [19] and ensuring the formation of the crystallographic structure of Nb/Au/YBCO heterojunctions with alternating transitions of the S/D_C and S/D_{45} type. Obtained YBCO films had a superconducting transition temperature $T_c = 87$–90 K and a critical current density of 10^4–10^5 A/cm² at $T = 77$ K [3, 4, 17]. The Au films were deposited in two stages: first by laser sputtering in situ in the same vacuum chamber at

[2] In view of the smallness of the superconducting current density in all hybrid heterojunctions studied, the condition for a lumped Josephson junctions was satisfied: the junction size L was smaller than the Josephson penetration depth λ_J for a magnetic field.

Sizes and electrophysical parameters of heterojunctions at $T = 4.2$ K

No.	L, μm	I_c, μA	R_N, Ω	V_c, μV	β_c	λ_j, μm
1	50	198	0.44	87	3	117
2	50	267	0.2	53	4	101
3	40	160	0.36	58	6	104
4	30	60	0.93	55	3	127
5	30	74	0.56	41	5	115
6	20	18	3.6	65	4	156
7	20	8.5	3.1	26	–	227
8	10	0.7	45.3	32	–	390
9	10	2.0	19.8	40	–	233

100°C, which minimized the decrease in the oxygen content and ruled out the effect of various impurities in the formation of the YBCO/Au two-layer structure. A test measurement of the superconducting transition temperature of the YBCO film after the formation of the YBCO/Au structure resulted in the value of $T_c = 89$ K for a superconducting transition width of $\Delta T < 0.5$ K. The formation of heterojunctions was completed by radiofrequency magnetron sputtering of an additional Au layer with a thickness on the order of 10 nm and a 200-nm-thick Nb film. Photolithography and ion-beam etching in argon were used for the formation of the geometry of square planar heterojunctions with an area $A = L^2$, where $L = 10$–50 μm [3, 4, 17]. In our opinion, the superconducting transition temperature of the YBCO film in completely prepared heterojunctions decreased to $T_c \approx 84$ K during the bombardment of the film by argon ions in the course of formation of the structure geometry. The superconducting transition temperature of Nb films was $T_c = 9.1$–9.2 K.

Electrophysical parameters of the films and heterojunctions were measured using a four-point scheme with a bias current in a temperature range of $T = 4.2$–300 K in magnetic fields $H < 50$ Oe under the action of electromagnetic radiation at frequencies $f_e = 36$–120 GHz.

3. ELECTROPHYSICAL CHARACTERISTICS OF HETEROJUNCTIONS

The Josephson effect was observed in all heterojunctions studied by us; the current–voltage (IV) characteristics of these heterojunctions did not display an excess current (Fig. 1). This circumstance indicates the absence of microshorts with direct conductivity, i.e., direct "short-circuits" between YBCO and Nb films, which usually lead to the emergence of excess current. In view of the small thickness of the Au interlayer, mutual diffusion of Nb and YBCO is possible. However, Nb/YBCO junctions have a very high characteristic resistance due to the formation of oxide layers of niobium. Additional measurements revealed that the characteristic resistance of Nb/YBCO junctions is $R_NA = 0.1$–1 Ω cm^2, which is several orders of magnitude higher than the characteristic resistance $R_NA = 10^{-6}$–10^{-5} Ω cm^2 of Au/YBCO junctions (R_N is the normal resistance). Using the values of R_NA, we estimated the transparency of the potential barrier at the Au/YBCO interface averaged over the area of the junction and over the directions of quasiparticles momenta; the resulting values of $\overline{D} = 10^{-5}$–10^{-4} are typical of superconducting tunnel junctions. It should be noted here that the resistance of the Nb/Au interface is substantially lower (by several orders of magnitude) than that of the Au/YBCO interface due to better matching of the Fermi velocity and the absence of chemical interaction of the materials [20].

The superconducting critical current density averaged over the area of the heterojunctions at $T = 4.2$ K is given by

$$\langle j_c \rangle = I_c/A = 1\text{–}10 \text{ A/cm}^2,$$

where I_c is the critical current. The values of the Josephson penetration depth λ_J for a magnetic field, which are calculated by the formula

$$\lambda_J^2 = \frac{\Phi_0}{2\pi\mu_0\lambda\langle j_c\rangle}, \quad (1)$$

where μ_0 is the permeability of vacuum, lie in the interval 100–400 μm and are much higher than the maximal linear size of the junctions studied here (see table). The quantity $\lambda \approx 220$ nm in formula (1) is the sum of the London penetration depths for YBCO and Nb. For the Nb/Au/YBCO heterojunctions studied here, the condition

$$L < 4\lambda_J \quad (2)$$

is satisfied; this condition implies that such heterojunctions must possess the properties of lumped Josephson junctions and the values of $\langle j_c\rangle$ and R_NA must be independent of the junction size L [21, 22].[3] However, the experimentally observed values of $\langle j_c\rangle$ and R_NA depend on the size of the heterojunctions (see inset b to Fig. 1). The increase in the values of R_NA observed upon a decrease in size $L \le 20$ μm indicates a decrease in the barrier transparency D, which may be due to an oxygen-depleted YBCO layer formed in regions near the

[3] For $L > 4\lambda_J$, a Josephson junction should be treated as a distributed structure in which dynamic processes are determined by the motion of Josephson fluxons.

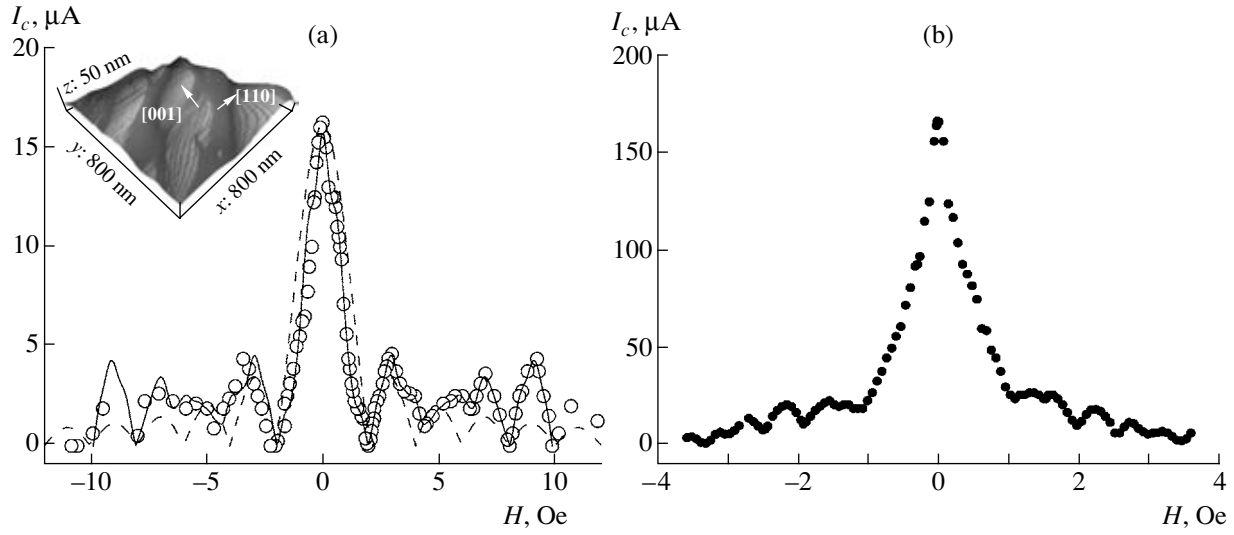

Fig. 2. Experimental magnetic field dependences of the critical current at $T = 4.2$ K for heterojunctions with sizes $L = 20$ μm (a) and 50 μm (b). The Fraunhofer dependence $|\sin H|/H$ is shown by the dashed curve. The solid curve is the calculated $I_c(H)$ dependence in the model of alternating density of the superconducting critical current. The inset shows the image of the (1 1 20) surface of the YBCO film, obtained using an atomic force microscope. The crystallographic orientations of the growth steps of the YBCO film are shown by arrows.

edges of the heterojunctions during sample preparation [20]. For junctions with a size $L < 40$ μm, the value of $\langle j_c \rangle$ increases in proportion to L and attains saturation for $L > 40$ μm. With increasing L, the contribution from the edge regions with a reduced value of $\langle j_c \rangle$ to the total superconducting current through the heterojunction decreases, and the edge effects can be disregarded even for $L = 30$ μm (see inset b to Fig. 1). It should be noted that the characteristic voltage $V_c = I_c R_N$ remains virtually unchanged upon a change in L, which is typical of tunnel junctions of S superconductors. For Josephson junctions based on high-T_c superconductors of metal-oxide materials, the value of V_c depends on $\langle j_c \rangle$ as a rule. For example, the value of V_c for bicrystal YBCO junctions is proportional to $V_c \propto \sqrt{\langle j_c \rangle}$ [2, 8], which is usually explained in the literature by the existence of different transport mechanisms for the superconducting and normal components of the current [9, 18].

4. MAGNETIC-FIELD DEPENDENCES OF THE CRITICAL CURRENT OF HETEROJUNCTIONS AND THEIR STRUCTURE

For heterojunctions with $L = 20$ μm, the experimental $I_c(H)$ dependence of the critical current on the magnetic field in the region of the first peak (Fig. 2a) is close to the "Fraunhofer" dependence $|\sin H|/H$ typical of lumped Josephson junctions with $L \approx 2\lambda_J$ [22]. It can be seen from Fig. 2a that as the magnetic field increases to $|H| > 5$ Oe, the deviation of the $I_c(H)$ dependence from $|\sin H|/H$ increases, indicating that the distribution of the superconducting current can be treated as quasi-uniform [8, 18]. A more accurate approximation of the experimental $I_c(H)$ dependences in the range of high fields $H \geq 5$ Oe can be obtained using a theoretical model in which the absolute value, as well as the sign of j_c, varies over the length of the junction [8, 10, 11, 23, 24]. It is impossible to unambiguously determine the distribution of the superconducting current density j_c in a junction from the experimental dependence $I_c(H)$. The evaluation of j_c gives at least several solutions that describe the $I_c(H)$ dependence in the region of peripheral peaks more exactly than $|\sin H|/H$. The experimentally measured $I_c(H)$ dependences can be approximated much better on the basis of alternating rather than unipolar distributions $j_c(x)$. The accuracy of calculations of $j_c(x)$ increases with expansion of the range of the experimental magnetic field, which was limited in our case by the trapping of magnetic flux quanta for $H \approx 10$ Oe. In stronger fields, a hysteresis loop was observed in the magnetic-field dependences and the dependences were poorly reproduced. In Fig. 2, we represent only reproducible unambiguous $I_c(H)$ dependences.

For junctions of larger size ($L > 30$ μm), the $I_c(H)$ dependence strongly differs from $|\sin H|/H$; in the region of the first peak, it resembles the dependences observed in distributed junctions, although condition (2) for lumped junctions is still observed (see Fig. 2b and table). It was shown theoretically in [10, 11] that the presence of a faceted interface in a Josephson junction, for which the conditions $\lambda \ll b \ll \lambda_J$ holds (b is the characteristic size of the facet), leads to the formation of "splintered" Josephson fluxons with a fractional magnetic flux quantum. The characteristic size λ_s of such a splintered Josephson fluxon for a one-dimen-

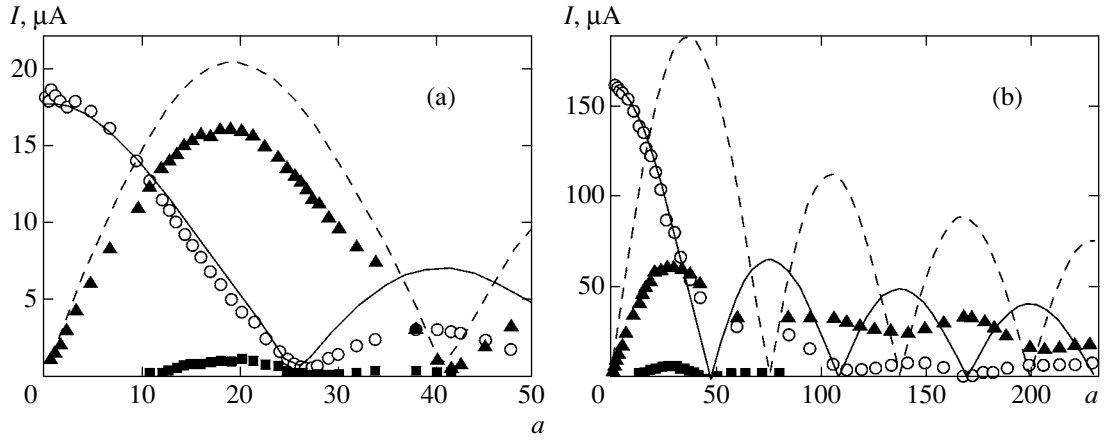

Fig. 3. Experimental dependence of critical current I_c (○), first I_1 (▲) and fractional $I_{1/2}$ (■) Shapiro steps on the dimensionless amplitude a of the high-frequency current $I_\sim$ for two heterojunctions at $T = 4.2$ K: (a) $L = 20$ μm, $f_e = 51.42$ GHz; (b) $L = 40$ μm, $f_e = 50.61$ GHz. The theoretical $I_c(a)$ and $I_1(a)$ dependences are shown by the solid and dashed curves, respectively. Calculations were made taking into account the second harmonic in the current–phase relation and the capacitance of the heterojunction (a) and in the framework of the RSJ (b).

sional dependence $j_c(x)$, which can be modeled by the expression

$$j_c(x) = \langle j_c \rangle + j_1 \sin(2\pi x/b),$$

can be estimated as

$$\lambda_s \approx \sqrt{2}\frac{\lambda_J^2 \langle j_c \rangle}{b j_1}, \qquad (3)$$

where j_1 is the amplitude of alternating modulation of the critical current density in the junction. For $j_1 \gg \langle j_c \rangle$, the fluxon size is small ($\lambda_s \ll \lambda_J$).

In our case, in view of the specific nature of deposition of YBCO films on inclined $NdGaO_3$ substrates with the (7 10 2) orientation, growth steps with a height of about 20 nm and a characteristic length of 200–300 nm in the plane of the substrate are present on the (1 1 20) surface of the YBCO films (see the inset to Fig. 2a and the results of atomic-force microscope measurements presented in [3, 4]). Such growth steps are mainly oriented along the (001) and (110) crystallographic planes of the YBCO film. According to the results of theoretical calculations [2, 5–7], the junctions with the (001) and (110) planes give different types of junctions (S/D_c and S/D_{45}, respectively) in view of the d symmetry of the order parameter in the YBCO film. It was shown earlier in experimental studies [17, 18] that the S/D_c junctions at $T = 4.2$ K can be treated as Josephson 0 junctions with a nonsinusoidal current–phase relation; in this case, the second harmonic amplitude amounts to about 10% of the critical current. As regards the S/D_{45} junctions, Andreev states with energies $\varepsilon \ll \Delta_D$ are formed in them in addition to Andreev states with $\varepsilon \approx \Delta_D$ on the order of the superconducting gap in a D superconductor like in S/D_c junctions [2, 8]. It was proved theoretically in [2, 5, 6, 8] that the stable state in the S/D_{45} Josephson junctions at helium temperatures is a state with a phase shift equal to π, with the characteristic voltage

$$V_c \approx \frac{\Delta_D^2 \overline{D}}{ekT}$$

and with a large second harmonic amplitude in the current–phase relation. Thus, due to the presence of alternating S/D_c and S/D_{45} junctions, the structure of the heterojunctions studied here has the form of a chain of parallel-connected 0 and π Josephson junctions.

In the heterojunctions studied so far, faceting predominantly occurs in only one direction [3, 5]; consequently, we can also use one-dimensional expressions in our case [10]. For example, using our estimates for j_1 and $\langle j_c \rangle$ we obtain from expression (3) $\lambda_s \approx 10$ μm for heterojunction no. 3 with $\lambda_J = 104$ μm, $\lambda = 0.22$ μm and $b = 0.2$ μm. It should be noted that the condition $\lambda \ll b$ which is used in calculations [10] does not hold exactly in our experiments; for this reason, the estimates of the value of λ_s based on formula (3) are correct only in order of magnitude. However, the other necessary condition for the existence of splintered fluxons [10, 11],

$$b \ll \lambda_J \sqrt{\frac{\langle j_c \rangle}{j_1}} \approx 1 \text{ μm},$$

is satisfied to a high degree of accuracy.

Experiments [11] show that splintered fluxons are unstable formations. In all probability, the instabilities on the IV curves and magnetic-field dependences of the critical current in large-size heterojunctions ($L > 40$ μm),

which were observed in our experiments, are precisely due to instability of such fluxon formations.

As a result, despite the strict fulfillment of condition (2), the magnetic-field dependences observed for the heterojunctions studied here are typical rather for distributed Josephson structures with an alternating distribution of the superconducting current density and a fluxon penetration size $\lambda_s < \lambda_J$.

5. DYNAMIC PROPERTIES OF HETEROJUNCTIONS

The IV curve presented in Fig. 1 was measured under the action of external monochromatic electromagnetic radiation with a frequency $f_e = 43.45$ GHz for $L = 40$ μm. It should be noted that the IV curve exhibits the first (I_1), second (I_2), and even fractional ($I_{1/2}$) Shapiro steps. An analogous form of the IV curve is also observed for heterojunctions with a size $L \geq 20$ μm. Figure 3 shows the dependences of the critical current amplitudes I_c and first Shapiro step I_1 on amplitude a of the high-frequency current $I_\sim$ normalized to the critical current ($a = I_\sim/I_c$). According to the results of calculations based on the resistive model of Josephson junctions (RSJ) [21, 22], the $I_c(a)$ and $I_1(a)$ dependences shown in Fig. 3a proved to be proportional to Bessel functions $J_n(a)$ for small-size heterojunctions with $L \leq 20$ μm. With increasing L, a considerable deviation of the experimental $I_c(a)$ and $I_1(a)$ dependences from those calculated in the RSJ is observed. For example, the difference between the first peak $I_{1\max}$ in the $I_1(a)$ dependence from the theoretical value calculated in the RSJ amounts to 25% for heterojunctions with $L = 20$ μm (Fig. 3a), while the deviation from the theory for heterojunctions with $L = 40$ μm is 70% (Fig. 3b). Figure 3b shows that the shape of the $I_c(a)$ and $I_1(a)$ dependences also changes as the size of junctions increases to $L > 20$ μm; this may be due to the enhanced effect of the second harmonic in the current–phase relation for large heterojunctions (with $L > \lambda_s$) [10, 11, 21, 22]. It should be noted that the amplitude of fractional Shapiro steps increases with junction size L and with the critical current.

Let us consider the frequency dependences of the maximal values of the amplitudes of the first harmonic Shapiro step $I_{1\max}(f_e)$ shown in Fig. 4 for junctions with $L = 20$ and 40 μm. For lumped Josephson junctions, the value of $I_{1\max}(f_e)$ is determined by the amplitude of the first harmonic of Josephson oscillation, which increases with frequency and attains saturation for $hf_e > 2eI_cR_N$ in accordance with the resistive model (solid curve in Fig. 4) [21, 22].

For junctions of S superconductors, the RSJ approximation disregarding the presence of a Riedel singularity for $V \approx \Delta_D/e$, which follows from the results of microscopic theory, correctly describes the available experimental data up to voltages (Josephson oscillation frequencies) corresponding to the superconducting gap $2\Delta/e$ (e.g., $\Delta_{Nb}/h \approx 700$ GHz for Nb) [22]. However, as can be seen from Fig. 4, the normalized value of $I_{1\max}/I_c$ in our experiment noticeably decreases even at a frequency $f_e > 40$ GHz, which is much lower than frequency Δ_{Nb}/h. It should be noted that the effect of the Riedel singularity in tunnel junctions of S superconductors is manifested in the increase in the ratio $I_{1\max}/I_c$ [25]. For large heterojunctions ($L = 40$ μm) the observed decrease in the ratio $I_{1\max}/I_c$ was stronger than for small heterojunctions ($L = 20$ μm).[4] The theoretical calculations performed in [13] for Josephson junctions of D superconductors reveal a weak frequency dependence of the superconducting current component up to frequencies Δ_D/h corresponding to the gap voltage and exceeding 1 THz. Consequently, in the framework of existing theories, the change in the value of $I_{1\max}/I_c$ must be small in the frequency range $f_e = 35$–80 GHz. A possible reason for the noticeable decrease in the values of $I_{1\max}/I_c$ with frequency may be energy pumping from the first harmonic of the current–phase relation, which determines the value of $I_{1\max}$, to the second harmonic for $L \geq \lambda_s$ [10, 11]. The effect of the nonuniform distribution of the external microwave current at natural resonance of heterojunctions on the dynamics of formation of the Shapiro step (and the value of $I_{1\max}$), which we observed earlier in distributed heterojunctions of S superconductors [26], cannot not be ruled out either. The resonance frequency of natural electromag-

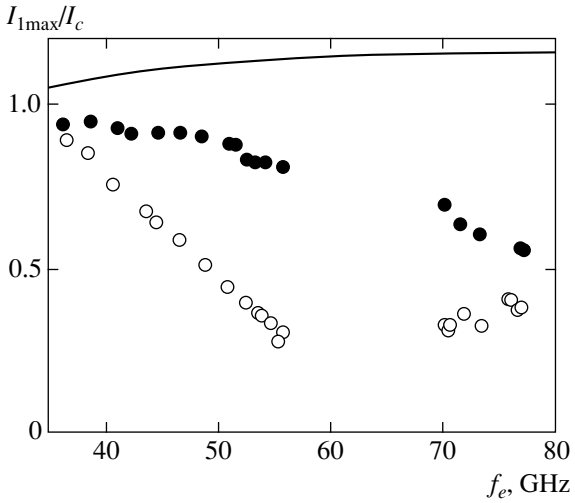

Fig. 4. Dependences of the normalized maximal amplitude of the first Shapiro step on the frequency of the external electromagnetic action for heterojunctions with $L = 20$ μm (dark circles) and 40 μm (light circles). The solid curve shows the frequency dependence of $I_{1\max}/I_c(0)$ calculate in the RSJ.

[4] Since the maximal value $I_{1\max}$ of the Shapiro step is measured, the frequency dependence of the heterojunction impedance, which affects the matching with the external system, can be ignored.

netic oscillations in the structures under study with a strongly nonuniform critical current density distribution may be close to the frequency of formation of standing waves. This effect is analogous to the Fiske resonance with the effective velocity of wave propagation on the order of $c_s = \omega_p \lambda_s$, where $\omega_p = \sqrt{2\pi I_c/\Phi_0 C}$ is the plasma frequency. As a result, the resonance frequency $f_s = c_s/2L$ turns out to belong, in order of magnitude, to the frequency range represented in Fig. 4. It should be noted that the IV curves did not display singularities corresponding to Fiske resonances.

6. SUPERCONDUCTING CURRENT–PHASE RELATION

It follows from Figs. 1 and 3 that the application of external monochromatic electromagnetic radiation to heterojunctions with $L = 20$–50 μm leads to the emergence of fractional Shapiro steps $I_{1/2}(a)$ in addition to harmonic steps on the IV curves at $V = (1/2)(hf_e/2e)$. For small-size heterojunctions ($L = 10$ μm), no fractional steps were detected; this is apparently due to the fact that the expected values of $I_{1/2\max}(a)/I_c(0) \le 0.1$ for these junctions were found to be smaller than the limiting current resolution of the measuring system (0.2 μA). A possible reason for the emergence of $I_{1/2}(a)$ steps on the IV curves of the heterojunctions is the deviation of the current–phase relation from the sinusoidal shape [3, 16]:

$$I_s(\varphi) = I_{c1}\sin\varphi + I_{c2}\sin 2\varphi.$$

It should be noted that the IV curves of the heterojunctions (both autonomous and those obtained under the action of an external electromagnetic field including those on which fractional Shapiro steps were observed) were symmetric about $V = 0$ in contrast to the IV curves for distributed Josephson junctions for $L > 4\lambda_J$ [27].

Higher harmonics in the current–phase relation ($\sin 2\varphi$, $\sin 3\varphi$, etc.) can be observed at low temperatures in Josephson junctions of the superconductor-normal metal-superconductor (SNS) type [21, 22]. Typical values of transparency for SNS junctions are $\overline{D} \sim 1$. However, the transparency values typical of our heterojunctions are $\overline{D} = 10^{-5}$–$10^{-4} \ll 1$, which enables us to treat them, rather, as tunnel Josephson junctions [3]; however, in contrast to the latter junctions, their current–phase relation is not necessarily sinusoidal.

Under the action of large-amplitude electromagnetic radiation (with $a \ge 1$), the quasiparticles energy distribution function may change, leading to the emergence of fractional Shapiro steps [28]. For this reason, we also measured the selective detector response of heterojunctions at frequencies $f_e = 35$–120 GHz at a small amplitude of electromagnetic radiation. Under these conditions, the detector response at voltages $V \approx (1/2)(hf_e/2e)$ corresponding to the emergence of the fractional Shapiro step $I_{1/2}(a)$ was observed for all junctions in which a step was detected. Thus, the emergence of the second harmonic in the current–phase relation in the form of fractional Shapiro steps was found to be independent of the amplitude of the external radiation. Indeed, the characteristic relaxation times for excited quasiparticles in superconducting metal-oxide materials are on the order of 10^{-13}–10^{-12} s [29], which is an order of magnitude smaller than the period of oscillations of external electromagnetic radiation in our experiments (10^{-11} s). Consequently, the quasiparticle energy distribution function remains close to equilibrium under the action of electromagnetic radiation with a frequency up to 100 GHz.

Deviations of the current–phase relation from sinusoidal shape (and, hence, fractional Shapiro steps) can be observed on the IV curves of distributed Josephson junctions in view of a nonuniform distribution of the superconducting current over the area of the junction (e.g., when condition (2) of a lumped junction is violated) [21, 22]. It was noted in Section 3 during the discussion of size effects that condition (2) holds for all heterojunctions studied by us. To find the effect of a nonuniform distribution of the superconducting current in a heterojunction on the current–phase relation, let us first consider heterojunctions for which a more stringent criterion for a lumped junction as compared to (2) is satisfied, i.e., $L < \lambda_s, \lambda_J$.

It was shown in Section 4 that the heterojunctions under consideration can be treated as a chain of Josephson 0 and π nanojunctions S/D_c and S/D_{45} in view of the (7 10 2) crystallographic orientation of the YBCO film and the morphology of its surface. It was noted above that the YBCO order parameter contains both *d*-symmetric and *s*-symmetric components, which are responsible for the emergence of current–phase relations of S/D_c and S/D_{45} nanojunctions of the first (I_{c1}) and second (I_{c2}) harmonics, respectively [17]:

$$I_{c1}R_N \approx \Delta_s\Delta_{\mathrm{Nb}}/e\Delta_D, \quad (4)$$

$$I_{c2}R_N \approx \overline{D}\Delta_{\mathrm{Nb}}/e. \quad (5)$$

In these expressions, we assume that the order parameter in YBCO is described by the expression

$$\Delta(\theta) = \Delta_D\cos 2\theta + \Delta_s,$$

where θ is the angle between the electron momentum and the direction of the *a* axis, and Δ_s is the *s* component of the order parameter. Taking into account the experimental transparency values $\overline{D} \approx 10^{-4}$, we obtain from expressions (4) and (5) the ratio of the amplitudes

of the harmonics in the current phase dependence,

$$q = \frac{I_{c2}}{I_{c1}} \approx \overline{D}\frac{\Delta_D}{\Delta_s} \approx 10^{-3},$$

for values of $\Delta_s/e \approx 1$ mV and $\Delta_D/e \approx 20$ mV typical of heterojunctions [3]. Such a level of deviation of the shape of the current–phase relation from sinusoidal cannot be detected at $T = 4.2$ K because of thermal fluctuations. At the same time, the contribution from Andreev levels to the superconducting current of S/D_{45} junctions leads to substantial increase in the second harmonic amplitude in the current–phase relation [2, 5]:

$$q \approx \frac{\Delta_D^3 \overline{D}}{kT\Delta_S\Delta_{Nb}kT} \approx 0.8.$$

A quantitative estimate of the contribution of the second harmonic in the current–phase relation to the height of the harmonic Shapiro step was obtained using the fact that the height of the nth harmonic step in the high-frequency RSJ approximation ($hf_e > 2eI_cR_N$) for $q \neq 0$ varies as the sum of Bessel functions J_n with different phases,

$$I_n/I_c = 2\max_{\Theta}[J_n(x)\sin\Theta + qJ_{2n}(2x)\sin 2\Theta], \quad (6)$$

where $x = a/\omega(\omega^2\beta_c^2 + 1)^{1/2}$; $\omega = hf_e/2eI_cR_N$ is the normalized frequency of the varying electromagnetic field; $\beta_c = 4\pi eI_cR_N^2C/h$ is the MacCumber parameter, which is determined by the capacitance C of the Josephson junction. The maximum of the expression in the brackets is taken for the phase shift Θ between Josephson oscillation and external radiation [21, 22, 30]. The values of the MacCumber parameter were obtained from the hysteresis on the IV curves for the heterojunctions under investigation and are given in the table; it can be seen that the value of $\beta_c = 3$–6 weakly depends on the size of the junctions. Expression (6) implies that the value of q at a frequency $hf_e > 2eI_cR_N$ can be calculated from the minima of the experimental dependence $I_c(a)/I_c(0)$. For example, at the first minimum, we have

$$q = \frac{I_c(a)}{I_c(0)J_0(2x)},$$

which gives $q = 0.14$ for the experimental dependence shown in Fig. 3a. It should be noted that this method of estimating q rules out the effect of the capacitance of the junction, but does not allow us to determine the sign of the second harmonic amplitude in the current–phase relation.

The finite capacitance of the junction and the second harmonic in the current phase dependence lead to the formation of fractional Shapiro steps on the IV curves with a height

$$\frac{I_{1/2}}{I_c} = 2\max_{\Theta}\left\{\sin\Theta\left[qJ_1(2x) + \beta_c\frac{J_1(x)J_0(x)}{(\beta_c\omega)^2/4 + 1} + 4q^2\beta_c\frac{J_2(2x)J_0(2x)}{(\beta_c\omega)^2 + 1}\cos\Theta\right]\right\}. \quad (7)$$

The expression in the brackets is sign-alternating; consequently, the $I_{1/2}(a)$ dependence differs from that obtained earlier for bicrystal junctions with a low capacitance [15]: $I_{1/2}(a) \propto J_1(2x)$, $x = a/\omega$. Values of $q < 0$ provide good agreement with experiment (Fig. 5). For $q > 0$, the calculated values of $I_{1/2}(a)$ substantially exceed the measured values and do not lead to the experimentally observed minimum between $a = 0$ and the first minimum of the $I_c(a)$ function. Negative values of q follow from theoretical calculations for S/D_{45} junctions [2, 5–7] and were observed earlier in experimental investigations of bicrystal Josephson junctions [9].

Pay attention to the fact that a slight change in the normalized frequency ω of the external radiation noticeably changes the shape of the $I_{1/2}(a)$ dependence. This is due to the simultaneous effect of the capacity of the junction and the nonsinusoidal current–phase relation on the process of formation of a fractional Shapiro step (the first two terms in expression (7) have opposite signs). The same behavior of the $I_{1/2}(a)$ dependence is also observed in our case (see Fig. 5), although the maximal value of $I_{1/2}(a)$ differs from the theoretical estimate by a factor of several units. It should be noted that we did not use any fitting parameters for comparing

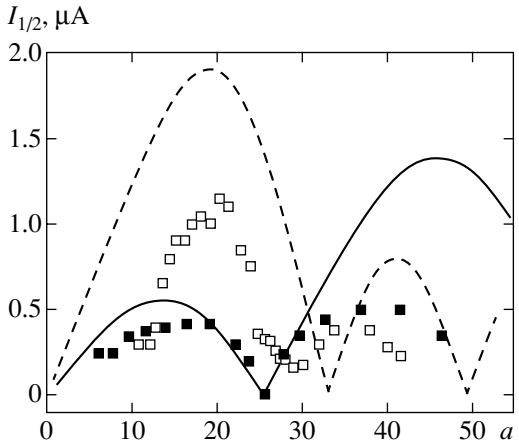

Fig. 5. Heights of fractional Shapiro steps $I_{1/2}$ for heterojunctions with $q = -0.14$ and $\beta_c = 4$ as functions of the normalized amplitude a of the external high-frequency current for frequencies $f_e = 51.42$ GHz (light squares) and 70.2 GHz (dark squares). The dashed and solid curves correspond to the $I_{1/2}(a)$ dependences calculated by formula (7) for normalized frequencies $\omega = 1.62$ and 2.2, respectively.

the experimental and theoretical results in Fig. 5. The second harmonic amplitude in the current–phase relation and the amplitude scale of external electromagnetic radiation were determined from comparing the results of calculation based on formula (6) with the experimental $I_c(a)$ dependence (see Fig. 3a).

According to [10, 11], the second harmonic amplitude $q \sim L^2/\lambda_s^2$ in the current–phase relation must increase with increasing size of heterojunctions ($L > \lambda_s$) due to the presence of parallel-connected 0 and π constants in the junctions. Indeed, the second harmonic amplitude $q = -0.4$ determined by formula (6) from the data presented in Fig. 3b for $L = 30$ μm increases to a value of $q = -0.9$ upon an increase in the junction size to $L = 40$ μm; in accordance with the results of calculations [11], all values of $q < 0$.

7. CONCLUSIONS

It was found from electrophysical and microwave properties of Nb/Au/YBCO thin-film hybrid heterojunctions that the critical current density in the junction is nonuniformly distributed over the junction length even for lumped junctions (which are smaller than the Josephson penetration depth, $L < \lambda_J$). Owing to faceting of the interface in Au/YBCO films and the effect of d symmetry of the superconducting order parameter in YBCO, the heterojunctions studied here are correctly described by the model of a chain of 0 and π junctions. In such chains, "splintered" Josephson fluxons can be formed with fractional values of the magnetic flux quantum and with values of λ_s several times smaller than the Josephson penetration depth for a magnetic field.

It was found experimentally that the maximal value of the first Shapiro step decreases with increasing frequency of external electromagnetic radiation. Such a behavior of high-frequency dynamic processes occurring at frequencies $f_e \ll \Delta_{Nb}/h$ may be due to the emergence of splintered fluxons leading to a nonuniform distribution of the magnetic and microwave fields in heterojunctions. This effect was enhanced with increasing junction size ($L > \lambda_s$); the departure of the magnetic-field dependence of the critical current from the Fraunhofer dependence also increased.

The fractional Shapiro step and the subharmonic selective detector response, which were experimentally observed in the heterojunctions studied here, are associated with the presence of the second harmonic in the current–phase relation. The second harmonic amplitude in the current–phase relation and its sign (the second harmonic amplitude is negative for heterojunctions under investigation) were estimated using experimental methods.

ACKNOWLEDGMENTS

The authors are grateful to I.V. Borisenko and I.K. Bdikin for their assistance in experiments, to Yu.S. Barash, V.V. Ryazanov, J. Mygind, T. Claeson, and F. Lombardi for fruitful discussions, and to É.B. Goldobin for a careful reading of the manuscript before publication and for helpful remarks.

This study was partly supported by the Russian Foundation for Basic Research (project no. 04-02-16818a), INTAS (grant nos. 2001-0809 and 2001-0249), OXIDE Program of the Swedish Foundation for Strategic Research (SSF, ISTC) (grant no. 2369), ESF Program "Pi-Shift," and the grant from the President of the Russian Federation supporting leading Science Schools (no. NSh-1344.2003.2).

REFERENCES

1. C. C. Tsuei and J. R. Kirtley, Rev. Mod. Phys. **72**, 969 (2000).
2. T. Lofwander, V. S. Shumeiko, and G. Wendin, Supercond. Sci. Technol. **14**, R53 (2001).
3. F. V. Komissinski, K. I. Constantinian, Yu. V. Kislinskiĭ, and G. A. Ovsyannikov, Fiz. Nizk. Temp. **30**, 795 (2004) [Low Temp. Phys. **30**, 599 (2004)].
4. F. V. Komissinski, G. A. Ovsyannikov, Yu. V. Kislinskiĭ, *et al.*, Zh. Éksp. Teor. Fiz. **122**, 1247 (2002) [JETP **95**, 1074 (2002)].
5. R. A. Riedel and P. F. Bagwell, Phys. Rev. B **57**, 6084 (1998).
6. Y. Tanaka and S. Kashiwaya, Phys. Rev. B **53**, R11957 (1996).
7. Yu. S. Barash, Phys. Rev. B **61**, 678 (2000).
8. H. H. Hilgenkamp and J. Mannhart, Rev. Mod. Phys. **74**, 485 (2002).
9. E. Il'ichev, M. Grajcar, R. Hlubina, *et al.*, Phys. Rev. Lett. **86**, 5369 (2001).
10. R. G. Mints, Phys. Rev. B **57**, R3221 (1998).
11. R. G. Mints, I. Papiashvilli, J. R. Kirtley, *et al.*, Phys. Rev. Lett. **89**, 067004 (2002).
12. E. Goldobin, D. Koelle, and R. Kleiner, Phys. Rev. B **67**, 224515 (2003).
13. Yu. S. Barash and A. A. Svidzinskiĭ, Zh. Éksp. Teor. Fiz. **111**, 1120 (1997) [JETP **84**, 619 (1997)].
14. L. H. Greene, P. Hentges, H. Aubin, *et al.*, Physica C (Amsterdam) **387**, 162 (2003).
15. G. A. Ovsyannikov, I. V. Borisenko, and K. Y. Constantinian, Vacuum **58**, 149 (2000).
16. E. Il'ichev, V. Zakozarenko, R. Ijsselsteijn, *et al.*, Phys. Rev. Lett. **81**, 894 (1998).
17. P. V. Komissinskiĭ, G. A. Ovsyannikov, E. Il'ichev, and Z. G. Ivanov, Pis'ma Zh. Éksp. Teor. Fiz. **73**, 405 (2001) [JETP Lett. **73**, 361 (2001)]; P. V. Komissinski, E. Il'ichev, G. A. Ovsyannikov, *et al.*, Europhys. Lett. **57**, 585 (2002).

18. R. Kleiner, A. S. Katz, A. G. Sun, *et al.*, Phys. Rev. Lett. **76**, 2161 (1996).

19. I. K. Bdikin, P. B. Mozhaev, G. A. Ovsyannikov, *et al.*, Fiz. Tverd. Tela (St. Petersburg) **43**, 1548 (2001) [Phys. Solid State **43**, 1611 (2001)].

20. F. V. Komissinskiĭ, G. A. Ovsyannikov, and Z. G. Ivanov, Fiz. Tverd. Tela (St. Petersburg) **43**, 769 (2001) [Phys. Solid State **43**, 801 (2001)].

21. K. K. Likharev and B. T. Ul'rikh, *Systems with Josephson Contacts: Foundations of Theory* (Mosk. Gos. Univ., Moscow, 1978) [in Russian].

22. A. Barone and G. Paterno, *Physics and Applications of the Josephson Effect* (Wiley–Interscience, New-York, 1982; Mir, Moscow, 1984).

23. N. V. Klenov, V. K. Kornev, I. I. Solov'ev, *et al.*, Nelin. Mir **3**, 75 (2005).

24. O. Nesher and E. N. Ribak, Appl. Phys. Lett. **71**, 1249 (1997).

25. D. A. Weitz, W. J. Skocpol, and M. N. Tinkham, Phys. Rev. B **18**, 3282 (1978).

26. B. Mayer, T. Doderer, R. P. Huebener, and A. V. Ustinov, Phys. Rev. B **44**, 12463 (1991).

27. A. V. Ustinov, J. Mygind, and V. A. Oboznov, J. Appl. Phys. **72**, 1203 (1992).

28. K. W. Lehnert, N. Argaman, H.-R. Blank, *et al.*, Phys. Rev. Lett. **82**, 1265 (1999).

29. J. Mannhart, Supercond. Sci. Technol. **9**, 49 (1996).

30. T. Y. Karminskaya and V. K. Kornev, in *Proceedings of International Students' Workshop on Microwave Applications of New Physical Phenomena* (St. Petersburg, Russia, 2004), p. 238.

Translated by N. Wadhwa